

Toward Generalization of Sub-Grid Turbulence Mixing Parameterizations in TC Models Using Observations

J.-W. Bao and C. Fairall

In collaboration with

S. A. Michelson, E. D. Grell,

S. G. Gopalakrishna, F. D. Marks, X. Zhang, J. Zhang

V. Tallapragada, Y. Kwon

NOAA/ESRL/PSD, NOAA/AOML/HRD, NOAA/NCEP/EMC

Purpose of this presentation:

Advocate using a coherent 3-D framework and observations to improve parameterized sub-grid turbulence mixing in TC models.

Outline

1. **Parameterizations of subgrid-scale mixing and PBL schemes in NWP models**
2. **Ongoing evaluation of the HWRF vertical subgrid-scale mixing (aka PBL physics) and the issues revealed**
3. **Preliminary results from testing a more generalized subgrid-scale mixing scheme in idealized simulations to deal with the above revealed issues**
4. **Future work**

1. Parameterizations of subgrid mixing and PBL schemes in NWP models

Reynolds-averaged Navier–Stokes equations: Basis for parameterizing 3-D subgrid mixing

- Grid scale filtering: $\Psi = \overline{\Psi} + \Psi'$ with $\overline{\Psi}(V, t) = \frac{1}{\Delta x \cdot \Delta y \cdot \Delta z} \int_V \Psi(V', t) dV'$
 $\overline{\Phi \Psi} = \overline{\Phi} \overline{\Psi} + \overline{\Phi' \Psi'}$ Volume balance approach (Schumann, 1975)
- The filtered equations of motion, e.g., in Boussinesq form

$$\frac{\partial \bar{u}_i}{\partial t} = -\frac{\partial \bar{u}_j \bar{u}_i}{\partial x_j} - \frac{1}{\rho_0} \frac{\partial \bar{\pi}^*}{\partial x_i} - \varepsilon_{ijk} f_j \bar{u}_k - \varepsilon_{i3k} f_3 \bar{u}_{gk} + \delta_{i3} \frac{g}{\theta_0} \bar{\theta}_v^* - \frac{\partial \tau_{ij}}{\partial x_j}$$

$$\bar{\pi}^* = \bar{p}^* + \frac{2}{3} \rho_0 \bar{e}, \quad \tau_{ij} = \overline{u'_i u'_j} - \frac{2}{3} \bar{e} \delta_{ij}, \quad \bar{e} = \frac{1}{2} \overline{u_i'^2}$$

Modified pressure

SGS stress

SGS TKE

What happened in most NWP model applications...

$$\frac{\partial \bar{u}}{\partial t} = -\bar{u} \frac{\partial \bar{u}}{\partial x} - \bar{v} \frac{\partial \bar{u}}{\partial y} - \bar{w} \frac{\partial \bar{u}}{\partial z} - \frac{1}{\rho} \frac{\partial p}{\partial x} - f\bar{v} + \mu \nabla^2 \bar{u}$$

2nd order

horizontal
subgrid mixing

$\frac{\partial \overline{u'u'}}{\partial x}$	$\frac{\partial \overline{u'v'}}{\partial y}$	$\frac{\partial \overline{u'w'}}{\partial z}$
---	---	---

$$\frac{\partial \bar{v}}{\partial t} = -\bar{u} \frac{\partial \bar{v}}{\partial x} - \bar{v} \frac{\partial \bar{v}}{\partial y} - \bar{w} \frac{\partial \bar{v}}{\partial z} - \frac{1}{\rho} \frac{\partial p}{\partial y} + f\bar{v} + \mu \nabla^2 \bar{v}$$

2nd order

Vertical subgrid mixing

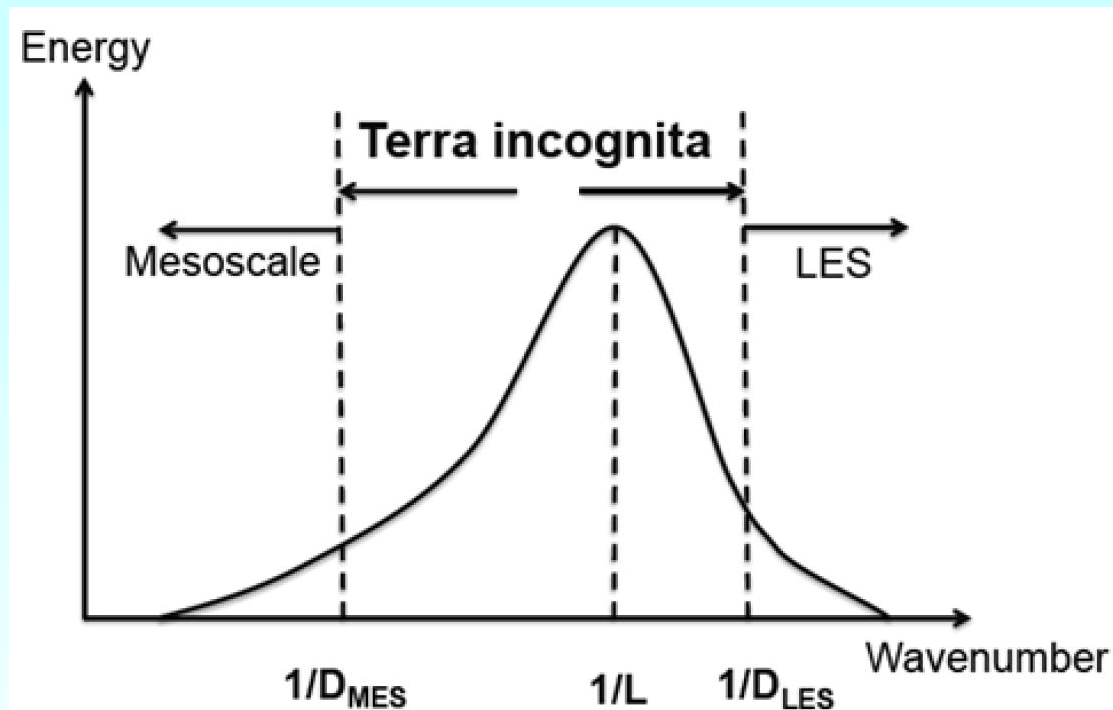
$\frac{\partial \overline{v'u'}}{\partial x}$	$\frac{\partial \overline{v'v'}}{\partial y}$	$\frac{\partial \overline{v'w'}}{\partial z}$
---	---	---

Horizontal subgrid mixing: resolved strain rate dependent, mostly numerical

Vertical subgrid mixing: stability depend, physically tied with the PBL mixing theory

There is no constraint on the conversion of grid-scale KE to subgrid TKE!

This diagram shows the form of the spectrum of turbulent energy. The peak energy occurs at a length scale L which gives an idea of a typical size of a turbulent eddy. In the atmosphere, this scale varies but is typically between a few tens of meters up to a kilometer.



It is still unresolved how to appropriately parameterize subgrid turbulent mixing when $D \sim L$. This is why it is called the “terra incognita” (Wyngaard 2004, JAS).

2. Ongoing evaluation of the HWRF vertical subgrid mixing (aka PBL physics) and the issues revealed

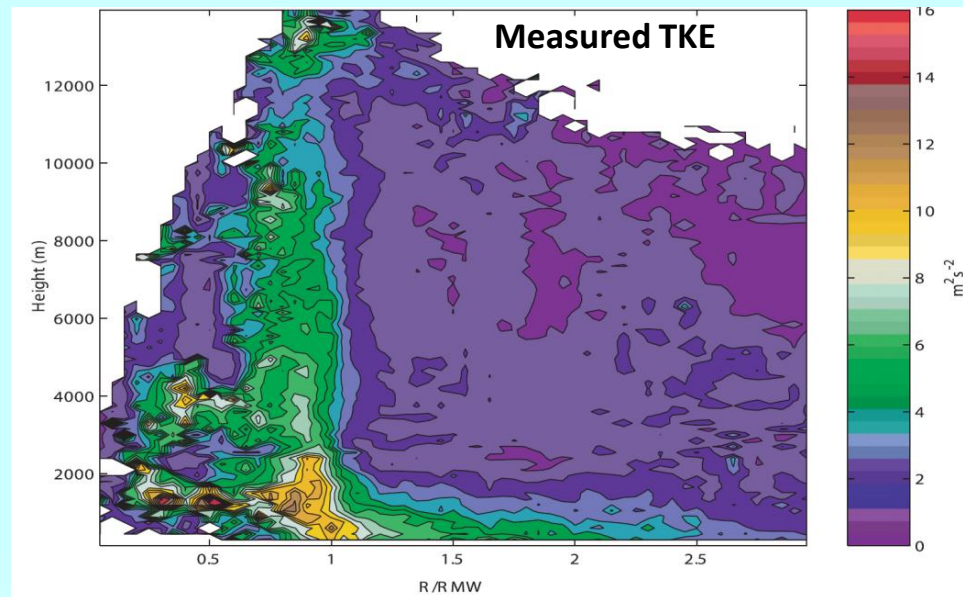
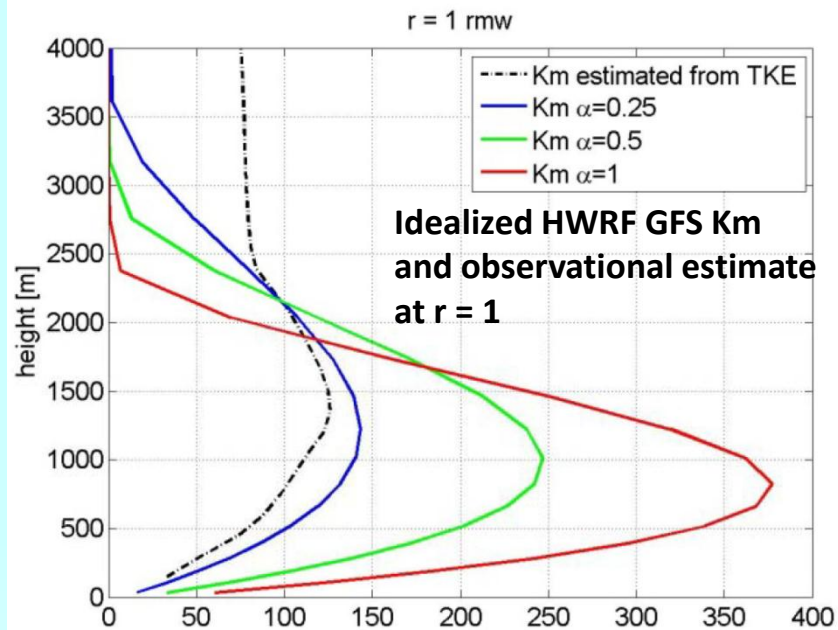
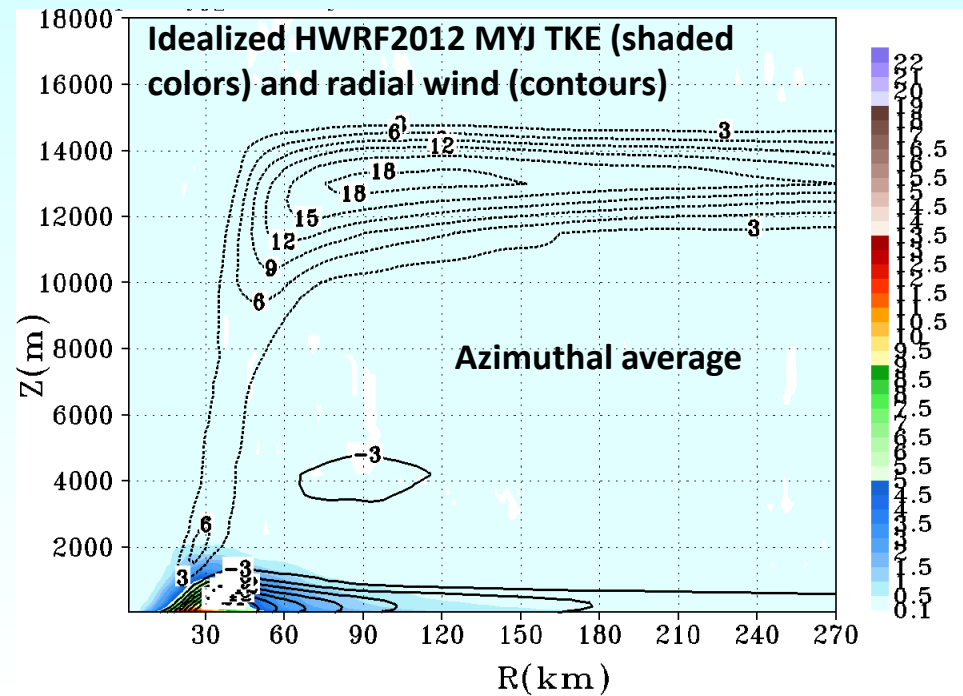
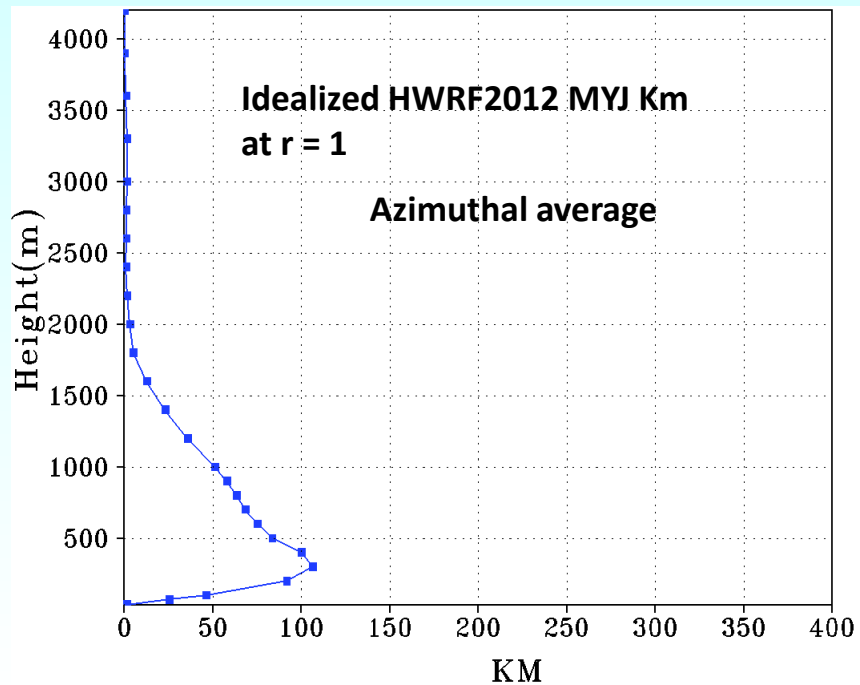


FIG. 7. The R - Z mean cross section of TKE for all cases, scaled on RMW.

Lorsolo *et al.* 2010



3. Preliminary results from testing more generalized subgrid mixing scheme in idealized simulations

Constraint on Grid Scale KE and Subgrid TKE Conservation (from G. Tripoli)

$$\begin{aligned}\frac{\partial k}{\partial t} &= \mathbf{V} \cdot \frac{\partial \mathbf{V}}{\partial t} \\ &= -\frac{1}{\rho} \nabla \cdot (\mathbf{V} \rho k) + \frac{k}{\rho} \nabla \cdot (\rho \mathbf{V}) - \mathbf{V} \cdot (\theta_{vw} \nabla \pi + \mathbf{g}) + \mathbf{V} \cdot (\mathbf{F}^1 + \mathbf{F}^2) \\ &= -\frac{1}{\rho} \nabla \cdot (\mathbf{V} \rho k) \quad + S_m^E \quad + S_h^{PV} \quad - S_e^{MP}\end{aligned}$$

1. flux divergence of k transport.
2. Change in kinetic energy resulting from elastic momentum convergence
3. Conversion from kinetic energy to thermal energy (work term) resulting from the nonhydrostatic pressure velocity correlation.
4. Mechanical production conversion to e (turbulence kinetic energy)

$$\frac{\partial e}{\partial t} = -\frac{1}{\rho} \nabla \cdot (\rho \mathbf{V} e) + F_e^1 + F_e^2 + S_e^{MP} + S_e^{BP} + S_e^{DS} + S_e^D + S_e^{BS}$$

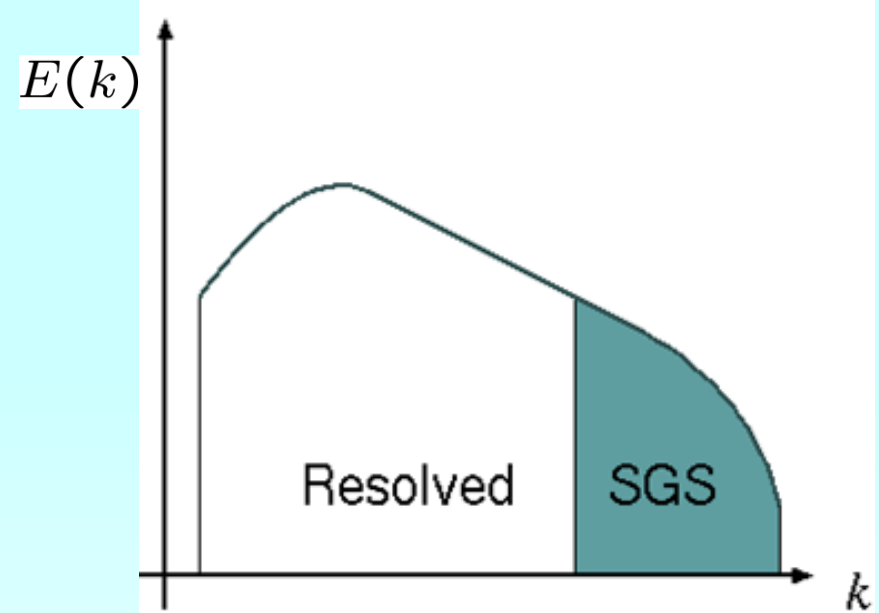
1. flux transport. The domain integral of this term produces a net source of e only from boundary fluxes
2. Physical turbulence
3. Numerical filter.
4. Mechanical production term
5. Buoyancy production term
6. Turbulence dissipation term- represents the downscale conversion of turbulence kinetic energy to molecular scale kinetic energy.
7. Divergence term
8. Mechanical backscatter production term.

Subgrid-scale parameterization (I): 3-D TKE closure

Introduce an SGS eddy viscosity, following the Boussinesq hypothesis

$$\tau_{ij} - \frac{\delta_{ij}}{3} \tau_{kk} \approx -2\nu_{sgs} S_{ij}$$

$$\underbrace{\bar{S}_{ij} = \frac{1}{2} \left[\frac{\partial \bar{u}_i}{\partial x_j} + \frac{\partial \bar{u}_j}{\partial x_i} \right]}_{\text{resolved strain rate}}$$



Express the eddy viscosity as the product between the velocity and length scale

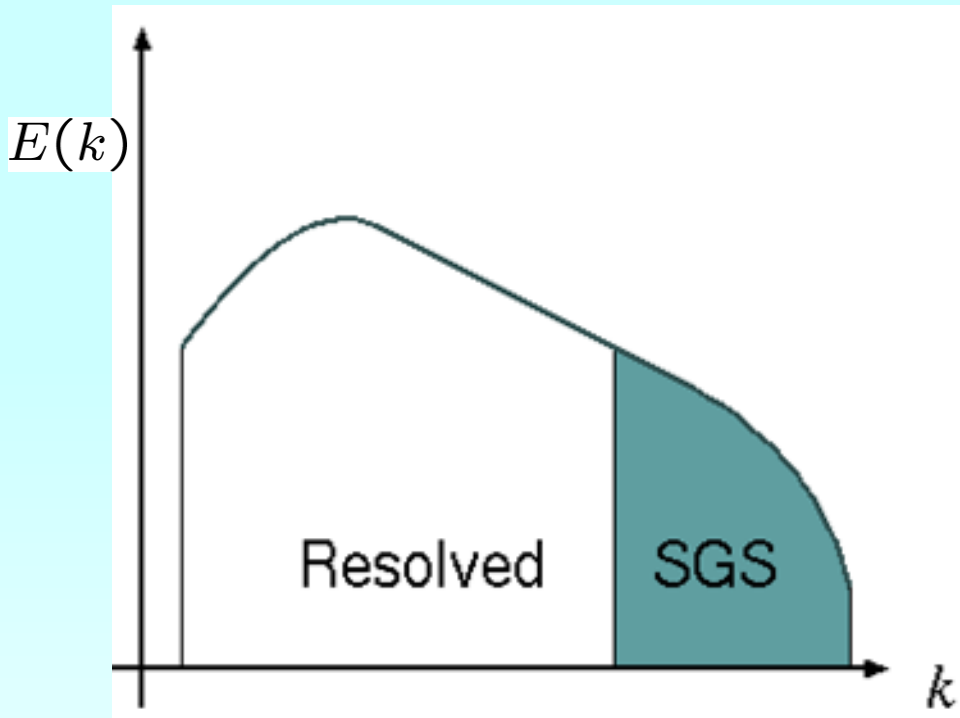
$$\nu_{sgs} \sim q_{sgs} l$$

q_{sgs} = square-root of twice the SGS energy

l = SGS length scale, usually the filter width

In high-resolution NWP models, the anisotropic nature of subgrid turbulence requires $L_h \neq L_v$.

Subgrid-scale parameterization (II): Smagorinsky closure



Production of SGS TKE: $-\tau_{ij}\bar{S}_{ij}$
balances viscous dissipation: ε_v

$$\varepsilon_v \approx q_{sgs}^3/l = q_{sgs}^3/\Delta$$

$$-\tau_{ij}\bar{S}_{ij} \sim q_{sgs}^3/\Delta$$

Leads to:

$$q_{sgs} \sim \Delta|\bar{S}| \quad |\bar{S}| = [2\bar{S}_{ij}\bar{S}_{ij}]^{1/2}$$

Obtain the Smagorinsky (1963) parameterization scheme
 (originally designed at NCAR for global weather modeling)

$$\nu_{sgs} \sim q_{sgs} l = (C_s \Delta)^2 |\bar{S}|$$

In high-resolution NWP models, $L_h \neq L_v$.

ARW Model Experiment Setup

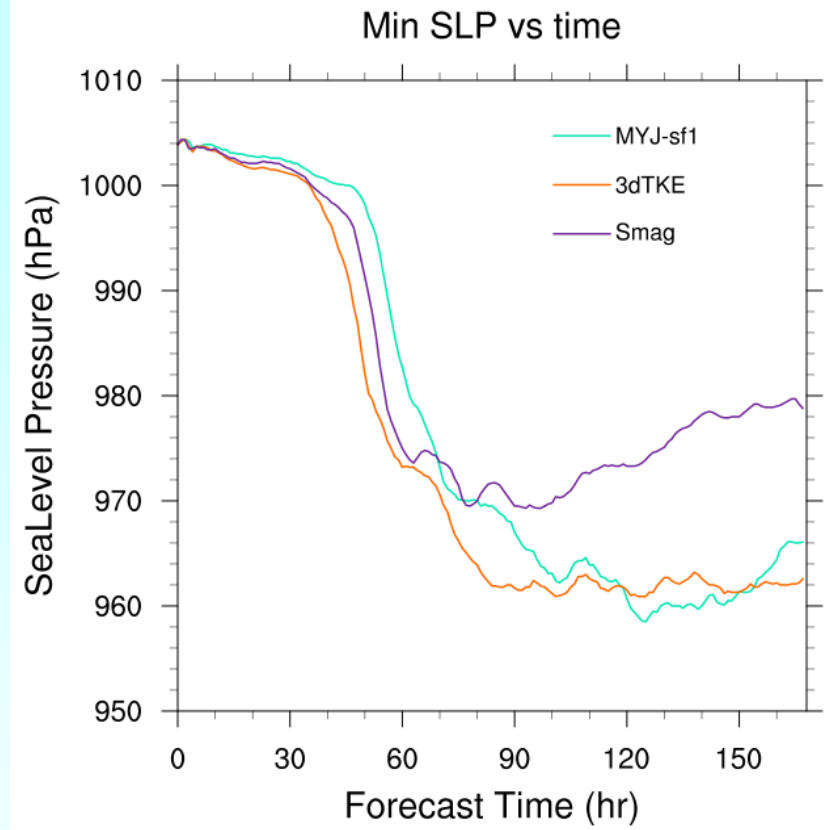
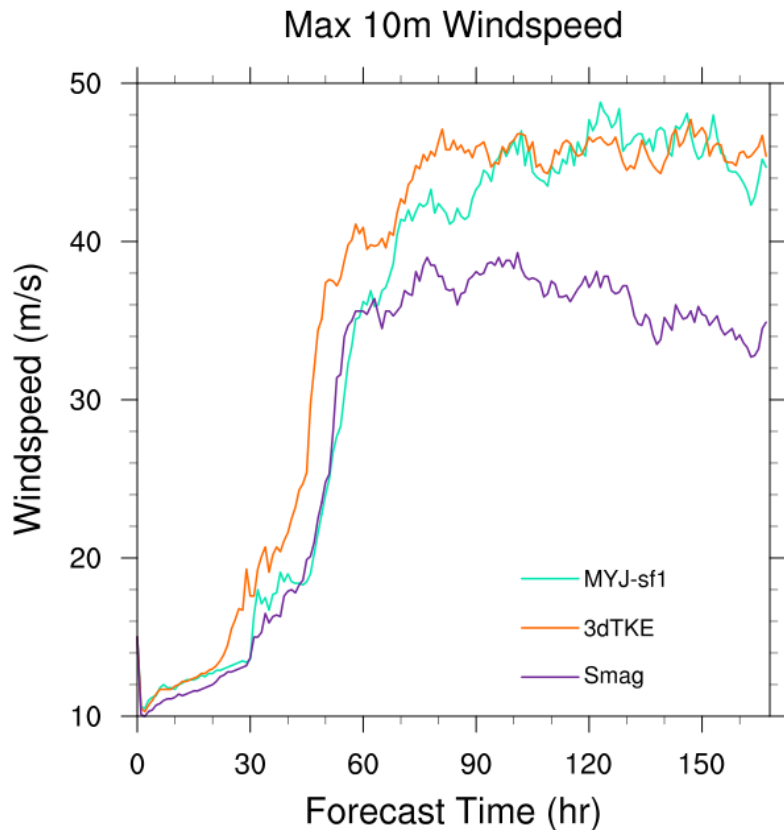
The model is initialized with a weak axisymmetric vortex disturbance in an idealized tropical environment that is favorable for the vortex disturbance to develop into a hurricane. The initial mass and wind fields associated with the weak vortex disturbance are obtained by solving the nonlinear balance equation for the given wind distributions of the initial vortex (Wang 1995, MWR), and the prescribed background thermal sounding and winds.

- f -plane located at 12.5°N
- The prescribed axisymmetric vortex:
 - maximum surface tangential wind: 15 ms^{-1}
 - radius of surface maximum wind: 90 km
- Quiescent environment thermally corresponding to the Jordan sounding with a constant sea surface temperature of 29°C
- Both models are run with 2 domains, a 9 km outer domain with a moving 3-km nest and 43 vertical levels

Table of experiments

Name of Experiments	V-Diff.	H-Diff.	Mixing Length	MP	CU	SFC
Sfclay1_MYJ_FerrSAS	MYJ	Smag+ TKE	$L_h = \Delta s$, $L_v = kz / (1 + kz / Linf)$ in PBL, and $L_v = \Delta z > PBL$	Ferrier	SAS (D1)	MO
sfclay1_stdwrf_FerrierSAS	3dTKE	3dTKE	$L_h = \Delta s$, $L_v = \Delta z$	Ferrier	SAS (D1)	MO
ssfclay1_mag_FerrierSAS	Smag	Smag	$L_h = \Delta s$, $L_v = \Delta z$	Ferrier	SAS (D1)	MO
Sfclay1_FerrSAS_cm1mods -linf100	3dTKE	3dTKE	$L_h = \Delta s$, $Linf = 100$ $L_v = kz / (1 + kz / Linf)$	Ferrier	SAS (D1)	MO
sfclay1_FerrSAS_10Lh_linf 100	3dTKE	3dTKE	$L_h = 10 * \Delta s$, $Linf = 100$ $L_v = kz / (1 + kz / Linf)$,	Ferrier	SAS (D1)	MO
sfclay1_FerrSAS_0.1Lh_linf 100	3dTKE	3dTKE	$L_h = 10 * \Delta s$, $Linf = 100$ $L_v = kz / (1 + kz / Linf)$	Ferrier	SAS (D1)	MO

Sensitivity to Diffusion Option (same surface layer scheme)

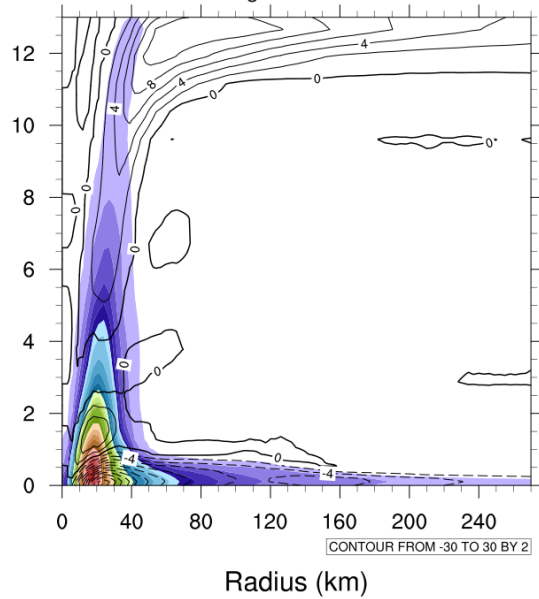


Sensitivity to Diffusion Option

Azimuthally averaged TKE and radial velocity

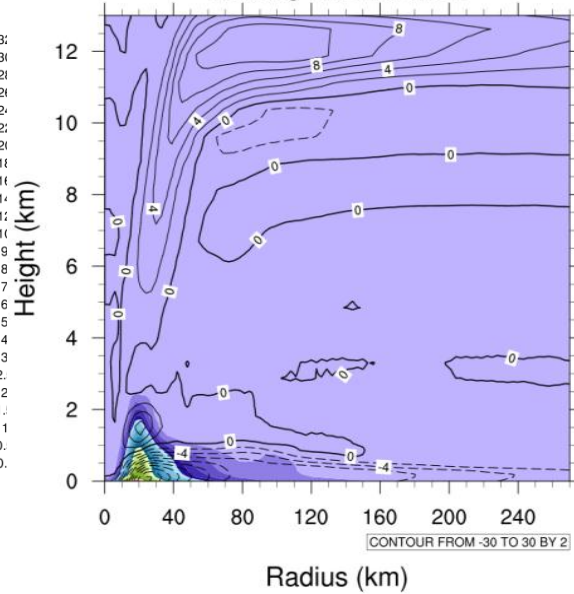
3km stdwrf_FerrierSAS tagv: 109-120h

Azim avg TKE and rad vel.

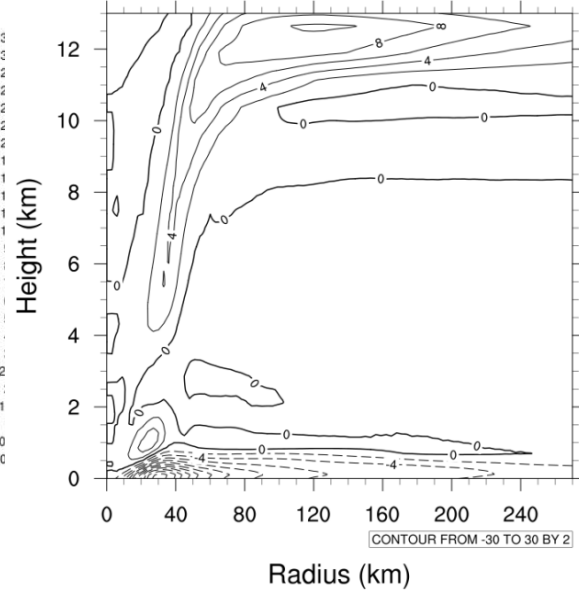


3km sfclay1_MYJ_FerrierSAS tagv: 109-120h

Azim avg TKE and rad vel.

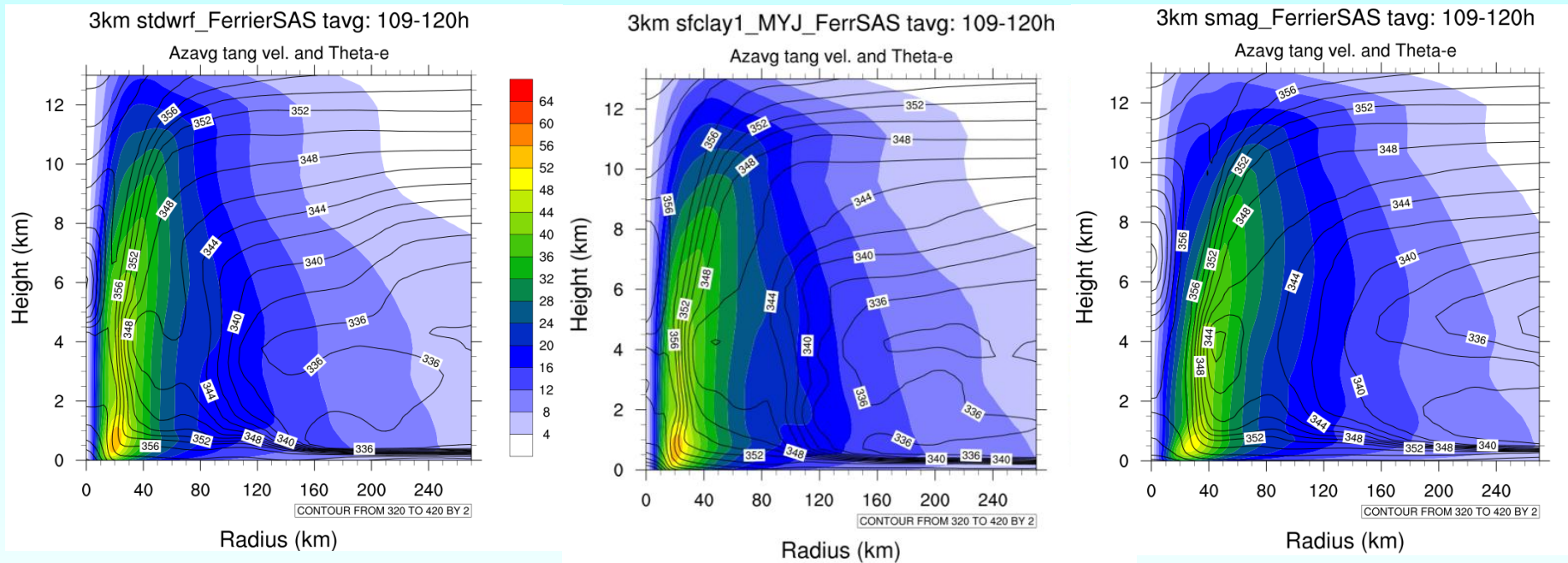


3km smag_FerrierSAS tagv: 109-120h



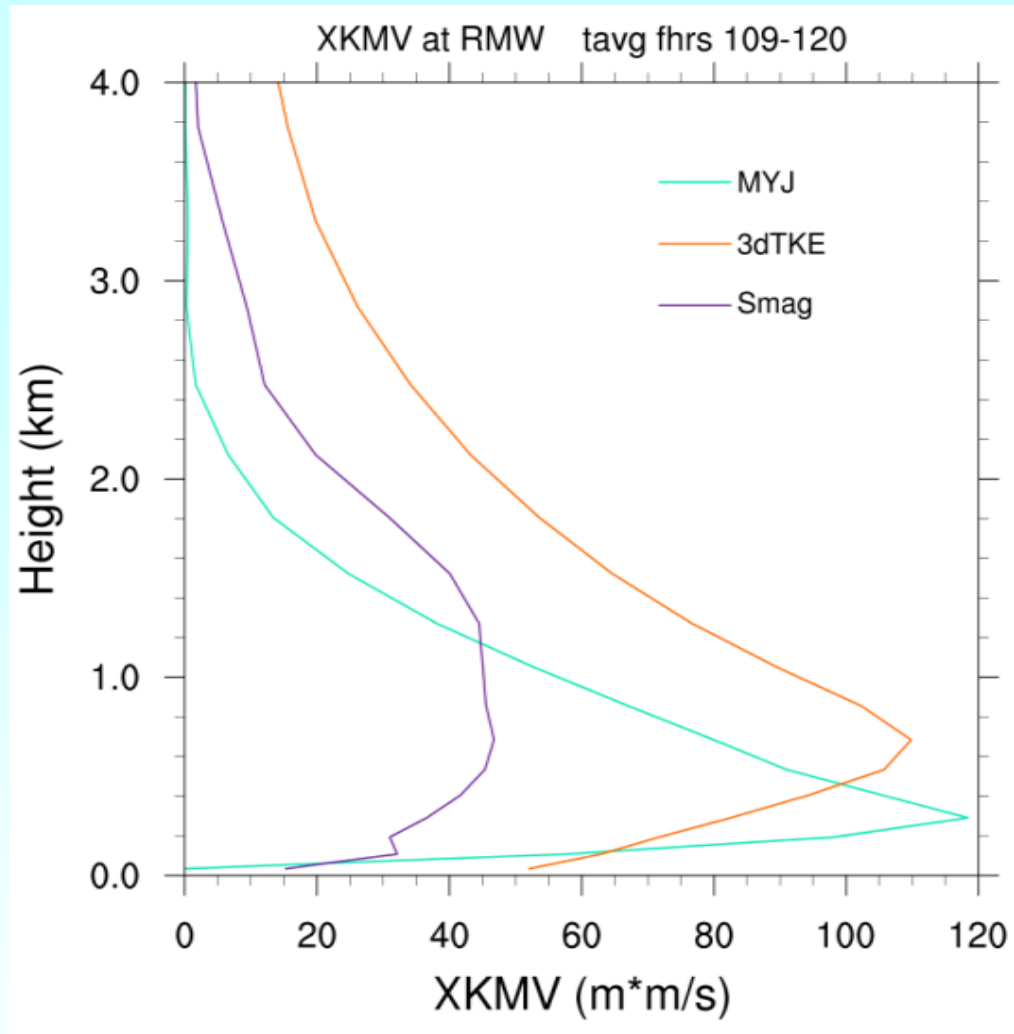
Sensitivity to Diffusion Option

Azimuthally averaged tangential wind speed and Θ_e



K Profiles at RMW

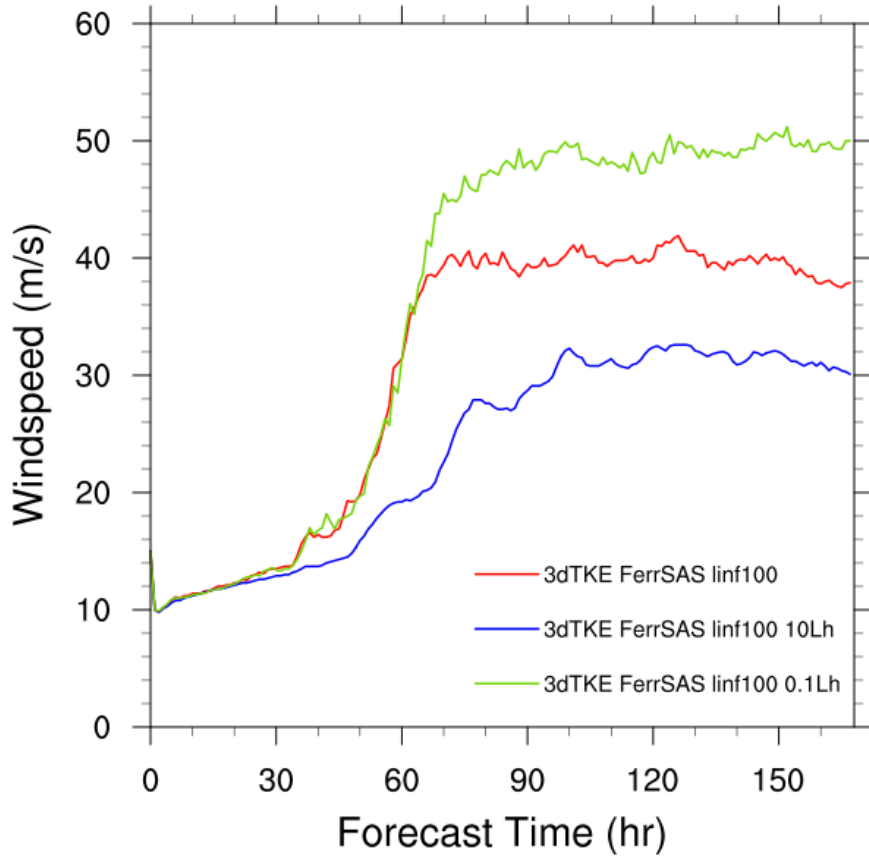
Varying diffusion options



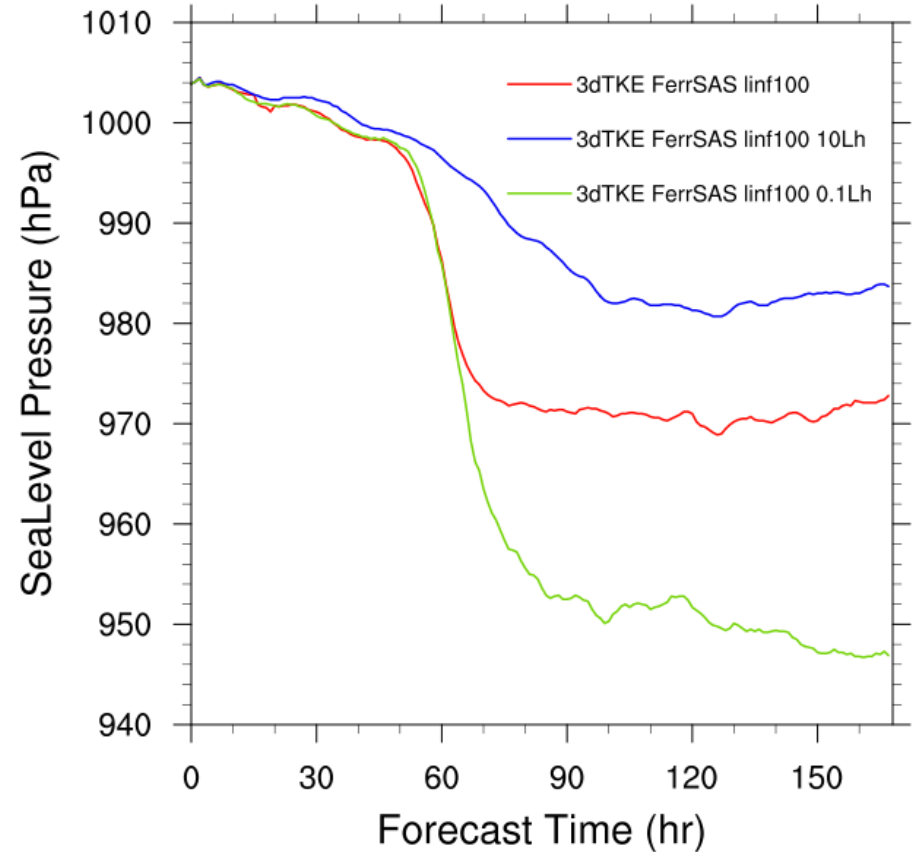
L_h sensitivity

$L_v = kz / (1 + kz / L_{inf}), L_{inf} = 100$

Max 10m Windspeed



Min SLP vs time

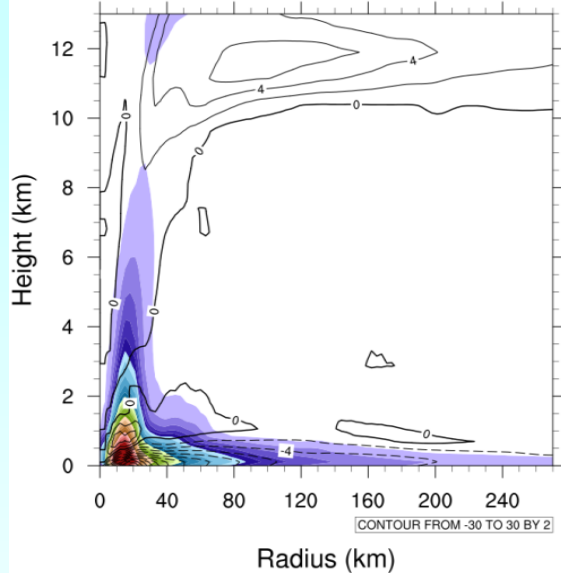


L_h sensitivity: $L_v = kz / (1 + kz / L_{inf})$, $L_{inf} = 100$

Azimuthally averaged TKE and radial velocity

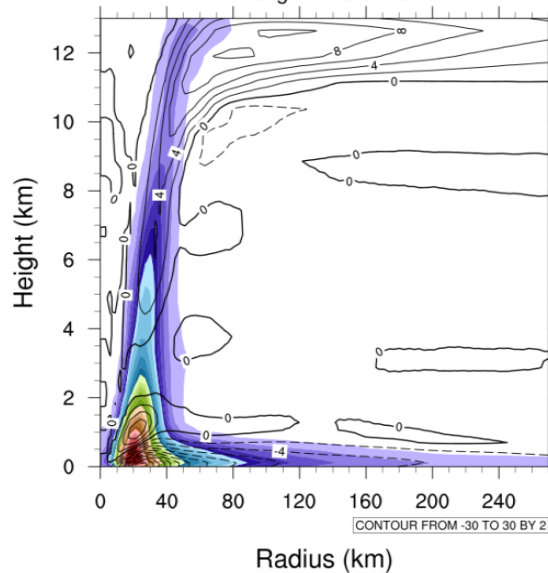
3km 3dTKE_FerrSAS_0.1Lh_linf100 tavg: 109-12

Azim avg TKE and rad vel.



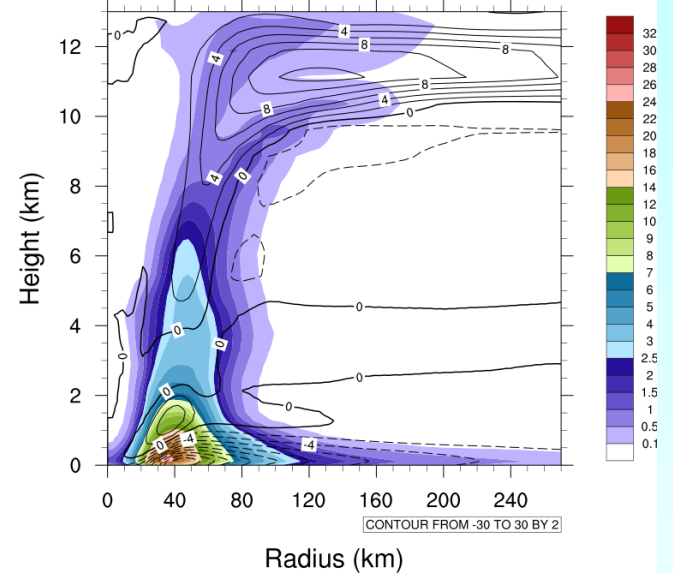
3km 3dTKE_FerrSAS-linf100 tavg: 109-120h

Azim avg TKE and rad vel.



3km 3dTKE_FerrSAS_10Lh-linf100 tavg: 109-120h

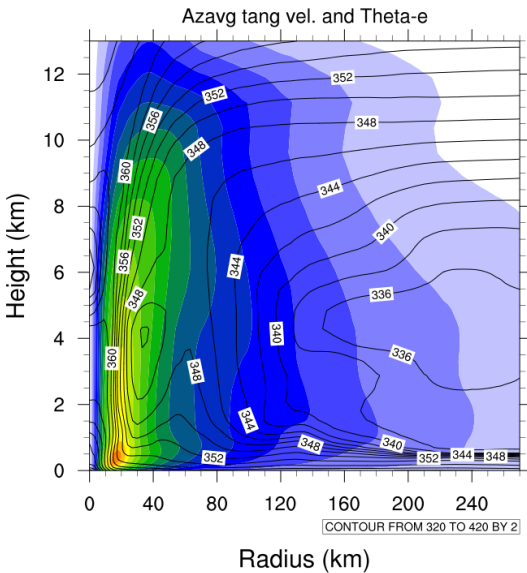
Azim avg TKE and rad vel.



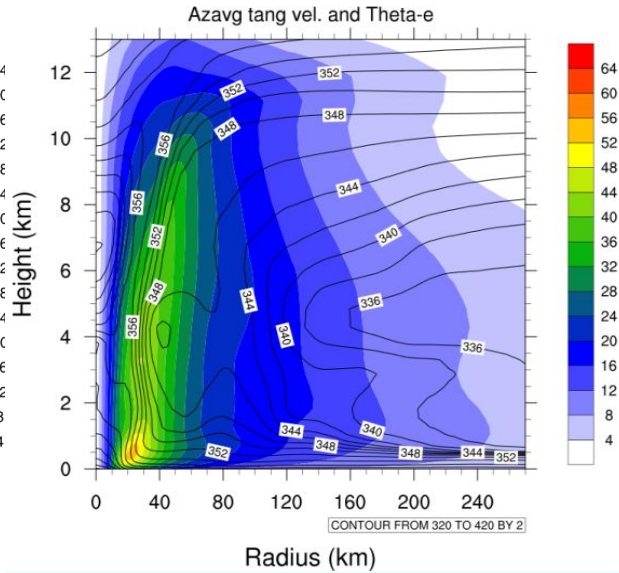
L_h sensitivity: $L_v = kz / (1 + kz / L_{inf})$, $L_{inf} = 100$

Azimuthally averaged tangential wind speed and Θ_e

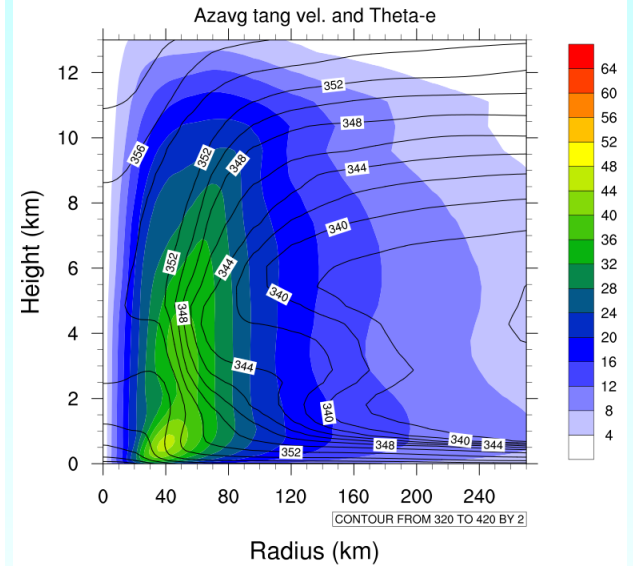
3km 3dTKE_FerrSAS_0.1Lh_linf100 tavg: 109-120h



3km 3dTKE_FerrSAS_linf100 tavg: 109-120h

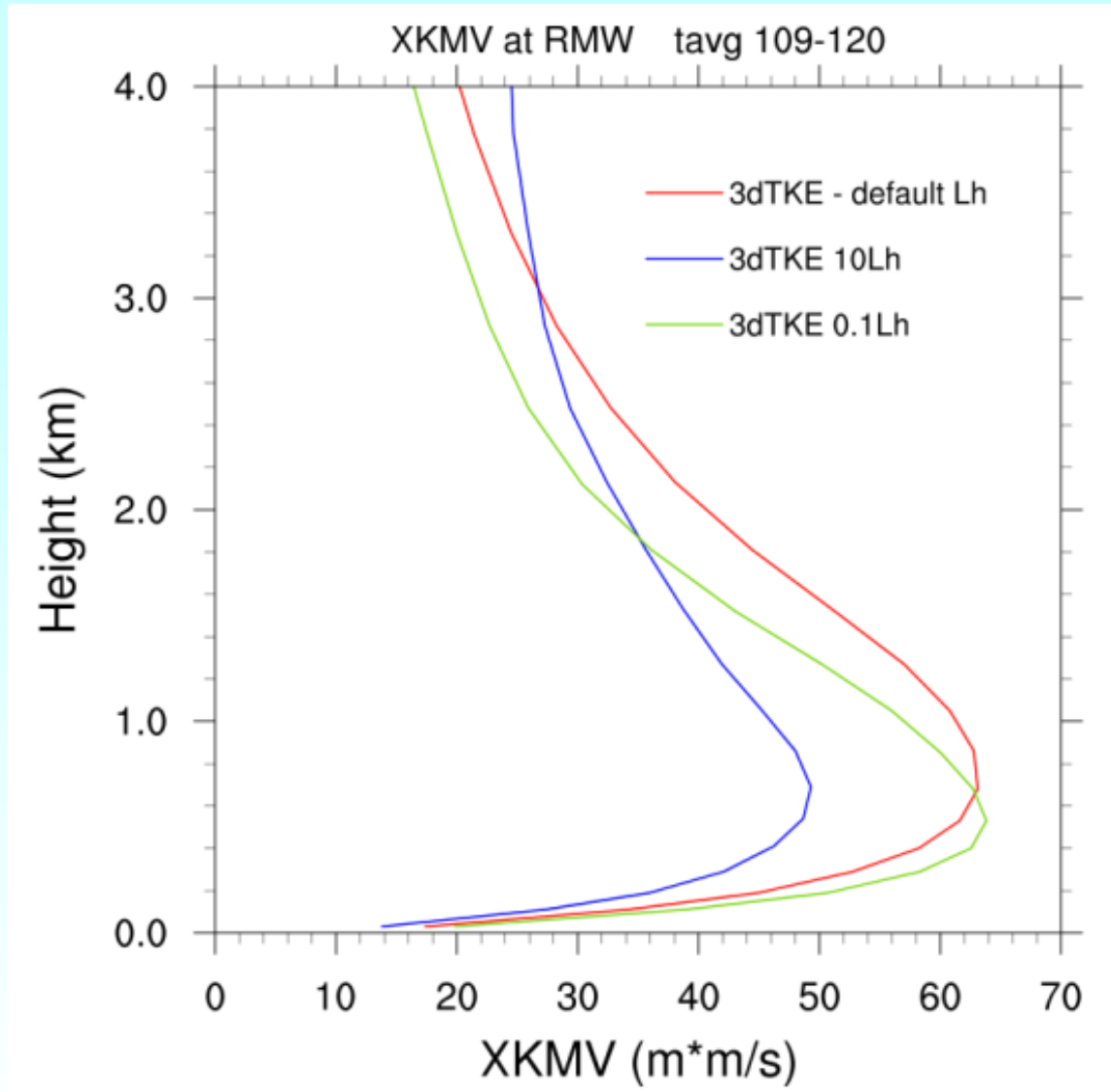


3km 3dTKE_FerrSAS_10Lh_linf100 tavg: 109-120h



K Profiles at RMW

Varying horizontal diffusion



Summary and Future Work

1. The conventional parameterizations of subgrid turbulent mixing in the HWRF are based on the H-V scale separation when horizontal grid spacing is much greater than the scale of PBL depth. No constraint in KE to TKE conversion.
2. Comparisons with the observational estimates indicate that the TKE in the MYJ scheme is underestimated above the BL inflow in the eyewall. While the results from the 3-D TKE scheme are consistent with the MYJ scheme in the BL inflow, the TKE is much greater than the MYJ scheme above the BL inflow .
4. **Coherent parameterizations of 3-D subgrid mixing should be adapted as the HWRF model resolution continues increasing.**
5. Comparisons of the model parameters describing subgrid mixing should account for the fact that the observational estimate of these parameters is scheme-dependent.
6. We will further evaluate the coherent 3-D framework for parameterizing subgrid turbulent mixing in the HWRF model using more observations.